American Research Journal of Biotechnology

Volume 1, Issue 1, 15-23 Pages
Research Article | Open Access

AMERICAN RESEARCH JOURNALS
An Academic Publishing House

# Based on Genome-Derived Minimal Metabolic Models of MG1655 Escherichia Coli, the in-Vivo Respiratory ATP Stoichiometry

**HuanLinyan, Yu Li, A. Malyska***

European Commission DG Research and Innovation, Brussels, Belgium.

## ABSTRACT

*Using this model, metabolic network models for E. coli growth on glucose, glycogen, and anaerobic substrates were constructed. The stoichiometry of energy generation and consumption in the metabolic network remains a mystery. Predicting the amount of biomass and the amount of products that can be made from that biomass is key to creating accurate projections. The E. coli network's unknown ATP stoichiometry values were estimated via eight experiments using E. coli MG1655, cultured at various dilution rates (0.025, 0.05, 0.1, and 0.3 h 1). Sugars (Glucose, glycerol and acetate), To accurately calculate the ATP stoichiometry, a precise biomass composition and net conversion rate estimate must be made under well-defined conditions. In order to build a biomass composition that is influenced by growth rate, observations and literature were employed It was found that an effective P/O ratio of 1.49 molar ATP to mole oxygen was predicted by metabolic network modeling, as was an effective growth-dependent maintenance rate of 0.46 molar ADP per C-mol of biomass and an independent growth rate (mATP) of 0.75-0.015 molar ADP/Cmol/h.*

*Escherichia coli has many important Herbert–Pirt connections and P/O ratios in the research.*

## INTRODUCTION

Cell signaling networks and their control are essential for the creation of new and better products that use industrial microorganisms or renewable resources, such as algae. This information is essential. Stoichiometric modeling has grown in popularity in the last decade as a technique for directing microbial metabolic engineering (Kim et al., 2008). To simulate stochastic processes, just the network's structure is required, not its unique biological activities. Biochemical and physiological data from the related organism may be utilized to build metabolic networks of the genome size (Durot et al., 2009). The metabolic model does not have to include all possible responses if certain well-defined variables of development are taken into consideration. Genome-scale response datasets may be reduced to specific metabolic network models using effective model reduction techniques, according to recent research (Burgard et al., 2001). According to Kayser et al., 2005, parameter values are typically determined using theoretical assumptions or in vitro studies (Kayser et al., 2005). For further information, see Varma and Palsson (1993). (Hempfling and Mainzer, 1975).

The ATP stoichiometry parameters may now be determined in real time thanks to Van Gulik and Heijnen's novel technique (1995). It is difficult to tell the difference between energy requirements that are growth-dependent and those that are not by using a constant rate of growth throughout all experiments. This experiment's parameters may be affected by limits on the kind of substrate used experiment. Cerevisiae growth on glucose/ethanol mixes, operational amino acid yields, and limitations on irreversibility (Van Gulik and Heijnen, 1995). Growth and penicillin production methods were used to study Penicilliumchrysogenum's metabolic network (Van Gulik et al., 2000). Carbon-restricted chemostat studies allowed the additional energy lost during b-lactam molecule synthesis to be determined. You may learn more by going to this website: (Van Gulik and colleagues, 2001). Stoichiometric models may reliably predict fluxes, growth, and product formation rates when the ATP stoichiometry coefficients are appropriately determined. Using such models, theoretical maximum biomass and product yields may be predicted based on stoichiometric and thermodynamic constraints. To effectively determine metabolic network stoichiometry, each microorganism must have a certain biomass composition. Using flux-based models, it has been shown that biomass composition affects flux distribution significantly (Pramanik and Keasling, 1998). When it comes to stoichiometry, we have never tested E. coli models in real-world circumstances. Carbon sources for E. coli MG1655 strain include glucose, glycerol, and acetate. Researchers employed the genome-scale model developed in 2003 in order to increase biomass output on a given substrate.

## COMPONENTS AND PROCESSES

### Stiffness and Growth Factors

Cultivated at 378 degrees Celsius and 220 revolutions per minute, precultures were fed a minimal medium containing 50% glycerol and grown under these conditions. It was necessary to neutralize the acidic solution created by the first pretreatment with 1 M K2HPO4 (FP 30/0,2 CA-S, 0.2-mm-pore size). Glucose, glycerol, and ethylacetate were utilized as a minimal medium in aerobic chemostat cultures that had carbon constraints. The dilution rates (D) used in glucose-limited chemostat tests varied from 0.025 to 0.01 hours 1. Dilution rates in acetate or glycerol-confined chemostats were as low as 0.01 hour 1. Fermenters with operational capacity of 4 liters and a volume of 7 liters were employed in all weight-controlled chemostat experiments (Applikon, Schiedam, The Netherlands). The following chemicals were utilized per liter in all chemostat experiments, except for the carbon source: trace element solution (Verduyn and colleagues, 1992), two milliliters of NH4Cl, and two milliliters of an antifoaming silicone-based antifoaming agent (Verduyn and colleagues, 1992). (BDH, Poole, United Kingdom). Researchers discovered that glycerol (75.8 mmol/L) and glucose (37.9, 75.8, or 151.5 mmol/L) are all carbohydrate sources, as was acetate (113.6 mmol/L). These plants were cultivated in media in a manner similar to how the medium was created and how the plants had previously been raised (TaymazNikerel et al., 2009).

**Table I**. Conditions (substance, concentration of substrate in feed vessel (CS,in), and rate of dilution D) and goal of the chemostat studies.

| Chemostat name | Substrate | $C_{S,in}$ (mM) | $D$ ($h^{-1}$) | Purpose |
|---|---|---|---|---|
| glu1 | Glucose | 37.9 | 0.102 | P |
| glu2 | Glucose | 37.9 | 0.099 | B, P |
| glu3 | Glucose | 37.9 | 0.314 | B, P |
| glu4 | Glucose | 37.9 | 0.049 | B, P |
| glu5 | Glucose | 37.9 | 0.025 | P |
| gly1 | Glycerol | 75.8 | 0.102 | P |
| gly2 | Glycerol | 75.8 | 0.099 | P |
| ace1 | Acetic acid | 113.6 | 0.097 | P |
| glu6 | Glucose | 75.8 | 0.100 | B |
| glu7 | Glucose | 151.5 | 0.102 | B |

Estimation of fluxes and parameter values; analysis of biomass composition When the DOT was less than 50%, there were no investigations to be done. In the feed medium, a chemostat culture is carried out before to the batch phase. Immediately after the end of a batch period in which CER and oxygen absorption rates rapidly decreased, medium feeding commenced (OUR). This was validated by off-gas studies of biomass concentration, carbon dioxide content, and dissolved oxygen content.

### Macromolecule and Element Composition in Biomass

The biomass of the organisms was harvested using E. coli cultures that had been deprived of glucose. A solution of 0.9 percent NaCl was used to rinse the cells for five minutes at 48 degrees Celsius (5,000 revolutions per minute). Biomass pellets were frozen at a constant temperature and pressure of 10 psi for 24 hours at an 808°C temperature (Edwards Modulyo, Sussex, UK). For the duration of the inquiry, it was defrosted and stored in a desiccator at room temperature.

### Calculating the Uptake/Sequestration Ratio is Crucial

For the culture filtrate, the carbon balance was calculated by determining the total carbon generated as dissolved components (TOC) in the culture (qlysis). "Unbalanced" conversion rates derived from raw data are what we use as our net conversion rates.

## PROPOSALS AND HYPOTHESES

### Oxidative Phosphorylation is a Characteristic of E

Activating the pmf in NDH2 does not result in the production of e 14 0. As well as references to Calhoun et al. (1993). Terminal oxidase H/E ratios are two for Bo-type and one for bd-type terminal oxidases. bd and bo types of terminal oxidases predominate when oxygen levels are low. Mate dehydrogenase seems to create PMF across the cell membrane, according to recent studies. In the respiratory chain, two protons are transported from formate to quinone, according to Ingledew and Poole (1984). It makes no difference how you respond since it has no effect. When exposed to oxygen, almost all of nonlim's constituents transform into to support the growth of organisms, ubiquinone-8 must be present in organisms' glycerol-3-phosphate dehydrogenase enzyme (Keseler et al., 2009). E. coli respiration's P/O ratio is governed by oxygen availability in its respiratory chain. Theoretically, an ATP synthase P/O ratio of 2 is possible with a H/ATP stoichiometry of 4. According to Stahlberg et al. (2001). Number of protons carried via system: This information is provided in Table II (see below).

### *Stoichiometry of ATP*

An equation for the metabolic network's ATP balance is given by

$$q_{\mathrm{ATP,ox}} - \sum q_i^{\mathrm{ATP}} - K_X\mu - m_{\mathrm{ATP}}=0, \qquad (1)$$

The metabolic network model's maintenance coefficients KX and mATP are growth-dependent and growth-independent, respectively (Van Gulik et al., 2001). The environment a person grows up in has an effect on how electrons travel through the respiratory chain. The facts in Table II may be used to explain oxidative phosphorylation.

$$q_{\mathrm{ATP,ox}} = \sum_{i=1}^{n} P/O^i q_{2e}^i \qquad (2)$$

**Table II.** Stoichiometry of proton translocation and maximum theoretical P/O ratio of each dehydrogenase involved in the *E. coli* metabolic network.

| Dehydrogenase | | Proton translocation | | Max P/O[a] | |
|---|---|---|---|---|---|
| NDH1 | NADH dehydrogenase | $8H^+/2e^-$ | 4+4 | 2 | $(\delta)$ |
| NDH2 | NADH dehydrogenase | $4H^+/2e^-$ | 0+4 | 1 | |
| SUCD4 | Succinate dehydrogenase | $4H^+/2e^-$ | 0+4 | 1 | $(\alpha_1\delta)$ |
| FDH2 | Formate dehydrogenase | $6H^+/2e^-$ | 2+4 | 1.5 | $(\alpha_2\delta)$ |
| DHORDT | Dihydroorotic acid dehydrogenase | $4H^+/2e^-$ | 0+4 | 1 | $(\alpha_3\delta)$ |
| G3PD5 | Glycerol-3-phosphate dehydrogenase | $4H^+/2e^-$ | 0+4 | 1 | $(\alpha_4\delta)$ |

[a]For the calculation of the maximal P/O ratios the $H^+$/ATP stoichiometry of the ATP synthase was considered to be equal to 4.

For E coil this can be expressed as

$$q_{ATP,ox} = \delta(q_{NDH} + \alpha_1 q_{SUCD4} + \alpha_2 q_{FDH2} + \alpha_3 q_{DHORD2} + \alpha_4 q_{G3PD5}) \quad (3)$$

The other dehydrogenases' contributions to proton translocation are shown by the letters A1 through A4, while d represents the NADH P/O ratio. Due to how they act together, it is difficult to discern patterns between the two.As a total, flow through both dehydrogenases is all that is taken into account (qNDH).

$$q_{ATP,ox} = \delta(q_{NDH} + 0.5q_{SUCD4} + 0.75q_{FDH2} + 0.5q_{DHORD2} + 0.5q_{G3PD5}) \quad (4)$$

### Estimation of Energetic Parameters Using CDR of All Data

Every chemostat experiment includes measurements of chemical concentrations, flow rates, and experimental errors. The metabolic network's key fluxes and covariance matrices can only be derived if the interaction matrix is known Linear regression is the technique of choice for calculating energy needs and oxidative phosphorylation efficiency (d) (Van Gulik et al., 2001).

Consequently, our reach has expanded. We estimate each node's fundamental flux balances using Equation 1 as an additional restriction. With the weighted sum of KX; mATP, it is possible to easily calculate each of the Chemostat experiments' weighed sum of squares. Each test's squared sums are combined together to arrive at an overall total.

$$SS_T(\delta, K_X, m_{ATP}) = \sum_{i=1}^{n} SS_i(\delta, K_X, m_{ATP}) \quad (5)$$

It is possible to compute d, KX, and mATP with the use of local curvature minimization. This objective's covariance matrix may be estimated via reducing local curvature. Under this method, the weight of each experiment is solely determined by its own measurements. The ATP balance is taken into consideration for the second time during our data reconciliation (Eq.1). As a starting point, we'll utilize this to figure out what the energy parameters are. Flux predictions have less room for error since the data support this idea.

## DISCUSSION OF THE FINDINGS

### Modeling of a Minimal Metabolic Network Based on the Genome

One process removes biosynthetic components and ATP from the network, representing an increase in biomass in this reconstruction. However, since biomass composition may be altered by growth rate, this method does not give an easy way to modify biomass composition. Protein, carbohydrate and fat, nucleic acid and DNA are all components of biomass that must be synthesised separately from each other.

This is why Reed etalgenome incorporated 14 more processes in their scale model in order to better represent (2003). The growth conditions and cells were discarded since no chemicals were present that could be employed for the 150 transport activities. There were 264 "dead-end" responses that had to be eliminated from the model. In the second step of the experiment, linear programming was used to optimize biomass output on the substrate. 276 non-zero flows were found as the only carbon source. the metabolic network model for aerobic glucose growth was reduced to its simplest form. Supplementary Material contains the whole answer set. As a contrast to the genome-wide optimum metabolic flux distributions for the three growth substrates, glucose, fructose, and sucrose, a reduced model was evaluated for its flux distribution (Edwards and Palsson, 2000). In the lower glycolysis, the TCA cycle, and the pentose phosphate pathway, the flux pattern was almost similar as a result. Unlike Edwards and Palsson (see Biomass Composition Section), we employed a biomass composition that deviated from our simplified model (2000). Glycerol and Acetate Growth Models Can Be Created Equivalently Using Catabolic Mechanisms in the Glycerol Growth Model (see Supplementary Material)

### How to Keep Chemostats in Good Condition

Chemostats may be used to develop new E. coli strains by changing the circumstances in which they grow (substrates and growth rates). Accordingly, we propose that the model's parameters be calculated by utilizing data from at least three independent sources. All of the chemostats with glucose limits (glu1–glu5) were run at the same 0.1-hour speed (0.05, 0.1, and 0.31 h 1). These measurements, which included biomass concentrations in offgases, oxygen and carbon dioxide concentrations, indicated that the cultures had stabilized after around five residence periods. No matter how few the nutrients were, all of the cultures continued to develop steadily. Glycerol and acetate-limited culture medium had 2.97 and 0.31 mg/L of glycerol and acetate left, respectively, according to the results of this investigation. All chemostat research may be calculated based on the observed concentrations of biomass and substrate, as well as

the flow rates of both liquid and gas. According to HPLC tests, these carbon-limited cells did not produce acetate, formate, lactate, or succinate. TOC levels in chemostat systems limited to acetate or glycerol were equal to those in systems only allowed access to glucose (15 and 13 mM, respectively).

**Table III** shows that E. coli cultivation rates (mmol/CmolX/h) at various dilution rates with various substrates (mmol/CmolX/h) are not in balance (uptake and secretion rates, per Cmol of biomass, qi, are imbalanced).

| Chemostat | $D$ ($h^{-1}$) | $C_X$ (g DW/L) | $q_X$ | $-q_S$ | $-qO_2$ | $qCO_2$ | $q_{lysis}$ | Carbon recovery | Redox recovery |
|---|---|---|---|---|---|---|---|---|---|
| glu1 | 0.102 | 2.90 ± 0.27 | 115.2 ± 2.7 | 30.6 ± 3.1 | 88.09 | 81.59 | 13.0 ± 1.4 | 107.0 | 115.3 |
| glu2 | 0.099 | 2.63 ± 0.05 | 113.7 ± 2.3 | 32.6 ± 1.3 | 97.09 | 87.54 | 14.53 ± 0.59 | 102.8 | 112.0 |
| glu3 | 0.314 | 2.99 ± 0.22 | 362.8 ± 8.1 | 93.6 ± 7.8 | 211.49 | 196.41 | 48.5 ± 4.1 | 99.5 | 105.4 |
| glu4 | 0.049 | 2.47 ± 0.10 | 58.8 ± 1.3 | 16.99 ± 0.90 | 61.46 | 51.05 | 9.38 ± 0.71 | 107.7 | 123.3 |
| glu5 | 0.025 | 1.96 ± 0.09 | 33.70 ± 0.78 | 10.73 ± 0.61 | 42.63 | 37.16 | 8.45 ± 0.54 | 110.1 | 123.8 |
| glyl | 0.102 | 2.91 ± 0.06 | 113.8 ± 2.3 | 60.3 ± 2.5 | 98.22 | 69.53 | 11.83 ± 0.46 | 101.4 | 104.6 |
| gly2 | 0.099 | 3.05 ± 0.09 | 110.2 ± 2.5 | 56.3 ± 2.6 | 94.70 | 65.83 | 11.1 ± 1.1 | 104.2 | 108.1 |
| ace1 | 0.097 | 1.44 ± 0.26 | 117.7 ± 4.5 | 176 ± 32 | 239.48 | 224.29 | 20.7 ± 3.9 | 97.2 | 101.2 |
| glu6 | 0.100 | 5.34 ± 0.07 | 114.1 ± 2.6 | 32.50 ± 1.2 | 88.69 | 87.30 | 14.0 ± 1.3 | 103.3 | 108.4 |
| glu7 | 0.102 | 10.24 ± 0.15 | 119.4 ± 2.6 | 33.55 ± 1.3 | 92.94 | 92.57 | 17.5 ± 1.3 | 105.3 | 109.9 |

Among the terms used are carbon dioxide production rate, biomass lysis rate, and biomass creation rate qX. It is obvious from carbon and redox recovery measurements (as well as lower levels of dilution) that the organic carbon found in the filtrate was generated by cell lysis (Taymaz-Nikerel et al., 2009). There is evidence of cell lysis, which indicates that the growth rate (m) isn't equal to the chemostat's dilution rate, but rather equal to the dilution rate plus the biomass-specific rate of cell lysis (qlysis). By failing to account for lysis, which results in a significant loss of ATP, inaccurate flow forecasts and incorrect coefficients will be generated. Calculated carbon and redox recoveries are shown in Table III. Overall, carbon recovery rates were within acceptable levels, as can be shown in this table Redox imbalances have been seen in various glucose-limited chemostats (recoveries up to 123 percent). Erroneous measurements of the offgas oxygen content are most likely to blame for the overestimation of oxygen absorption. During aerobic glucose-restricted growth in our chemostat cultures, however, oxygen intake exceeded carbon dioxide generation. In the ensuing data reconciliation and parameter estimate phase, oxygen readings that were out of wack were not utilized.

Various carbon, hydrogen, oxygen, nitrogen, and sulfide concentration in freeze-dried biomass samples were examined. Regardless of the rate of growth or the amount of substrate in the feed reported in Table IV, the feed's elemental compositions remained constant. We observed that the quantities of carbon and nitrogen were exactly in line with what had been previously reported.

| Chemostat code | $D$ ($h^{-1}$) | $C_{S,in}$ (mM) | C (%) | H (%) | N (%) | O (%) | S (%) |
|---|---|---|---|---|---|---|---|
| glu4 | 0.049 | 37.9 | 44.36 ± 0.08 | 7.57 ± 0.03 | 11.81 ± 0.02 | NA | 0.41 ± 0.01 |
| glu6 | 0.100 | 75.8 | 43.91 ± 0.05 | 7.29 ± 0.04 | 12.25 ± 0.01 | 28.36 ± 0.29 | 0.58 ± 0.02 |
| glu2 | 0.099 | 37.9 | 43.46 ± 0.06 | 7.35 ± 0.05 | 12.06 ± 0.01 | 27.66 | 0.47 ± 0.003 |
| glu2 | 0.099 | 37.9 | 45.09 ± 0.01 | 7.43 ± 0.03 | 12.38 ± 0.01 | 29.17 | 0.50 ± 0.03 |
| glu7 | 0.102 | 151.5 | 45.47 ± 0.03 | 7.63 ± 0.02 | 12.42 ± 0.03 | NA | 0.47 ± 0.01 |
| glu3 | 0.314 | 37.9 | 43.71 ± 0.03 | 7.34 ± 0.04 | 11.93 ± 0.03 | NA | 0.45 ± 0.02 |
| Average | | | 44.33 ± 0.33 | 7.44 ± 0.06 | 12.14 ± 0.10 | 28.40 ± 0.44 | 0.48 ± 0.02 |

Aerobic development is dependent on the availability of glucose (Bratbak and Dundas, 1984; Han et al., 2003; Heldal et al., 1985). The most acceptable approach was determined to be averaging the observed elemental compositions for various rates of growth and substrate concentrations in the diet. The average elemental composition was CH2:01N0;23O;48S0:004 (gx 14 4.37). 93% of the biomass is made up of these substances. Ash content refers to the quantity of phosphorus and other metal ions that are still present in the ash. An RQ of between 1.03 and 1.11 for dilution rates of 0.09–0.22 h yields between 1.93 and 3.00 Cmol biomass/mol glucose in aerobic glucose restricted E. coli K12 cells. Several studies were published in 2002, including Emmerling and colleagues, Fischer and Sauer, Hua et al. (Hua and colleagues 2003), and Johansson et al. (Johansson et al.). Based on biomass yields, E. coli was determined to have a gx of 4.23–4.41. This may be found in the appendix. gx of 4.37 falls inside this range.

## Macromolecular Compound Structures

On glucose minimal medium, the biochemical content of E. coli B/r was examined at 378C (a mass-doubling duration of 40 minutes). RNA accounted for 20.5% of the mass, while DNA accounted for 3.1%, while lipids accounted for 9.1%, while lipopolysaccharides accounted for 3.4%, while peptidoglycan accounted for 2.5%, and glycogen (14polysaccharide (PS) accounted for 2.5% of the mass. Protein accounted for 55.5% of the mass, while RNA and DNA each accounted for 2.5%. Macromolecules previously measured were utilized, however the composition of Neidhardt (1987) was employed for molecules not previously quantified. Environmental and growth factors have been shown to change biomass macromolecular composition (Bremer and Dennis, 1996). By measuring protein content in glucose-limited chemostats, we found that the protein content did not vary appreciably with changes in specific growth rate. A high degree of agreement was found between the measured protein content and previously reported values (Table V) (Table V). It was decided to use Table V (Emmerling et al., 2002). The rate of growth of the organism should be taken into account while determining RNA concentration. The RNA/DNA ratio was used to estimate the DNA concentration (Neidhardt, 1987). Pramanik and Keasling investigated

the amino acid composition in an aerobic chemostat with glucose limitation (1998). E. coli proteins were shown to have minor differences across strains and/or growing conditions. When it comes to DNA's concentration of deoxyribonucleic acid (DNA), growth rate has minimal influence (Pramanik and Keasling, 1998). There was a precise ratio allocated to each of the remaining organic biomass components such as LPS and PG and putrecine as well as the spermidine and putrescine (Neidhardt, 1987). Ash content was believed to be independent of growth rate for elemental analysis reasons as well. Although the average elemental composition was projected to be CH2:01N0:23O0:48S0:004 in Table IV, it was actually CH2:01N0:23O0:48S0:004 that was found to be the actual composition. This suggests a significant decrease in biomass if the biomass's elemental and biochemical components vary significantly.

**Table V** shows the protein and RNA concentrations of E. coli in aerobic glucose-limited chemostat cultures (as a percentage of dry weight).

| *E. coli* strain | $D$ ($h^{-1}$) | Protein (%) | RNA (%) | References |
|---|---|---|---|---|
| JM101 | 0.09 | 69.8 | 7.2 | Emmerling et al. (2002) |
| JM101 | 0.4 | 61.7 | 15.4 | Emmerling et al. (2002) |
| K12 W3110 | 0.1 | 70 | 7 | Hua et al. (2003) |
| K12 MG1655 | 0.12 | 70.1 | 4.7 | Fischer and Sauer (2003) |

meaning to indicate that the other party is mistaken Biomass declines at a rate higher than 4.2% only for lipids (in Cmol). Cells growing at a tenth the rate of our chemostats should have a higher lipid content than Neidhardt's 9.1%. (1.0 h 1). (in the range of 0.03–0.4 h 1). The quantities of hydrogen and oxygen in the elemental composition altered when fat was added to the biological composition. The most probable reason is water remaining in the freeze-dried biomass. Prior to this experiment, yeast samples had showed this kind of behavior (Lange and Heijnen, 2001). There are macromolecular and elemental compositions of biomass at growth rates ranging from 0.025% to 0.3% in Table VI (right). Data reconciliation and parameter estimation were made easier with the aid of the models described above. Neidhardt's biomass composition (4.22) is a nice instance of this, since it follows the observed trend of gx falling as growth rate increases (see Table VI). A high biomass harvesting growth rate (late exponential phase) in reality isn't a surprise to us at this point. Combined data reconciliation and energetic parameter estimation in a single process.

This method can accurately predict all three ATP stoichiometry parameters if the elemental conservation laws and the best estimations of crucial measurements and net conversion rates are satisfied (d, KX, mATP). The growth rate and carbon source have been examined to see whether they have a significant influence on the values of these parameters. Although four alternative growth rates might exist, a universal variable KX and mATP were used. Each of the three variables, including growth rate and carbon source, was given its own set of computations. Three universal ATP parameters beat the other models in all six circumstances.

**Table VI** shows the macromolecular biomass of E. coli when grown in an aerobic glucose-limited culture.

| | $D=0.025\,h^{-1}$ | $D=0.05\,h^{-1}$ | $D=0.1\,h^{-1}$ | $D=0.3\,h^{-1}$ |
|---|---|---|---|---|
| Protein | 63.95 | 64.81 | 68.19 | 65.43 |
| RNA | 5.21 | 5.86 | 7.26 | 13.06 |
| DNA | 0.79 | 0.89 | 1.10 | 1.98 |
| Total lipids | 20.18 | 18.80 | 14.54 | 11.20 |
| glyc | 6.30 | 5.87 | 4.54 | 3.49 |
| etha | 3.79 | 3.53 | 2.73 | 2.11 |
| hdca | 4.34 | 4.04 | 3.12 | 2.41 |
| hdcea | 3.33 | 3.10 | 2.40 | 1.85 |
| ocdcea | 2.42 | 2.26 | 1.74 | 1.34 |
| Lipopolysaccharides | 1.18 | 1.10 | 0.85 | 0.65 |
| Polysaccharide = glycogen | 0.87 | 0.81 | 0.62 | 0.48 |
| Peptidoglycan = murein | 0.87 | 0.81 | 0.62 | 0.48 |
| Putrescine | 0.40 | 0.37 | 0.29 | 0.22 |
| Spermidine | 0.13 | 0.12 | 0.10 | 0.07 |
| Ash | 6.43 | 6.43 | 6.43 | 6.43 |
| Sum | 100.00 | 100.00 | 100.00 | 100.00 |
| Biomass composition | $CH_{1.74}N_{0.24}O_{0.34}S_{0.006}P_{0.005}$ | $CH_{1.73}N_{0.24}O_{0.35}S_{0.006}P_{0.005}$ | $CH_{1.69}N_{0.25}O_{0.35}S_{0.007}P_{0.007}$ | $CH_{1.64}N_{0.27}O_{0.37}S_{0.007}P_{0.012}$ |
| $\gamma_x$ | 4.41 | 4.38 | 4.31 | 4.21 |

The percentage of cell dry weight that each It has been suggested that macromolecules are involved in the process. Our institution performed a little quantity of protein analysis. The RNA concentration was calculated using information from Table V. The DNA concentration of the sample was measured using Neidhardt's RNA/DNA ratio (1987). There are a number of fatty acids found in lipids, such as glycerol and ethanolamine as well as the C16:0 and C16:1 fatty acids hdca and hdcea, as well as the C18:1 fatty acid ocdcea. It was predicted that the ash content will continue at 6.43 percent over the long term.

**It's time for Table VII.**

qi given as mmol/CmolX/h per Cmol of biomass absorption and secretion rates for E. coli growth at various dilution rates in carbon-limited chemostats (reconciled).

| Chemostat | $q_X$ | $-q_S$ | $-q_{O_2}$ | $q_{CO_2}$ | $q_{lysis}$ |
|---|---|---|---|---|---|
| glu1 | 116.0±2.7 | 33.3±0.7 | 74.7±1.2 | 83.6±1.5 | 13.9±0.8 |
| glu2 | 113.0±2.5 | 32.51±0.65 | 73.4±1.2 | 82.0±1.4 | 14.22±0.51 |
| glu3 | 365.1±8.5 | 95.9±2.1 | 192±4 | 210±4 | 50.6±2.1 |
| glu4 | 59.0±1.4 | 18.82±0.37 | 48.3±0.7 | 53.9±0.8 | 9.8±0.7 |
| glu5 | 34.5±0.9 | 12.52±0.22 | 37.1±0.4 | 40.6±0.5 | 9.29±0.47 |
| gly1 | 113.7±2.5 | 61.2±1.2 | 91.6±1.5 | 69.8±1.1 | 11.89±0.36 |
| gly2 | 110.2±2.7 | 59.5±1.3 | 89.5±1.6 | 68.2±1.2 | 11.3±1.1 |
| ace1 | 116.3±2.9 | 162±4 | 199±4 | 208±4 | 19.2±1.2 |

For example, "biomass generation rate qX" is one phrase used to describe the rate at which carbon dioxide is produced from biomass.

With a P-value of 58% or above, no carbon source or growth rate was ruled out in the corresponding F-test. The bo-type terminal oxidase and the NDH2 dehydrogenase, which are not involved in the formation of PMF, may be detected in high concentrations of oxygen in the culture (see Theoretical Aspects Section). Close to the projected value of 1.49, the expected values range from 0.001 – 0.002.

At 2.81 moles/gram protein/hour (Kayser et al., 2005) and 2.81 moles/gram protein/hour, it's reasonable to infer that the mATP value calculated here is close to earlier estimations (Kayser et al., 2005). Affirmative (Farmer and Jones, 1976). Both the growth independent and growth dependent metrics for E.coli K12 MG1655, which was determined to have 8.4 mg/kg of dry weight per hour, were identified in the E.coli K12 MG1655. Growth-independent maintenance parameters of 3.2 0.7 mmol/g/h and 19.8 12 mg were substantially higher than these values, we found. A P/O ratio that is much higher than what we expected may have been utilized by Feist and colleagues (2007) because they used previously published data from many distinct E. coli strains cultured on a variety of basic medium. Our knowledge of the P/O ratio they employed in their computations should have been known to us. Compared to previous studies using S. cerevisiae and P. chrysogenum, our E. coli results are very distinct (Van Gulik and Heijnen, 1995). Cerevisiae and P. chrysogenum are all yeasts. In contrast to P. chrysogenum, E. coli had a growth-independent maintenance coefficient twice as high as the growth-related one. Biomass yield from a substrate may be calculated using estimated energy parameters and a metabolic network model. Substrate-based biomass generation is shown in Figure 1. The experimental yields on substrate were quite close to the expected values for all of the different growth conditions that were investigated. ATP coefficients are unaffected by growth rate or substrate, and we can now be certain that this remains true after these studies.

The stoichiometry parameters of the E. coli metabolic network ATP stoichiometry and comparisons to previously published data are shown in Table VIII (Van Gulik and Heijnen, 1995). In the year 2001, Van Gulik and coworkers The ATP stoichiometry of S. cerevisiae and P. chrysogenum were utilized to mimic the E.

| | $\beta$ (mol ATP/½ mol $O_2$) | $K_X$ (mol ATP/CmolX) | $m_{ATP}$ (mol ATP/CmolX/h) |
|---|---|---|---|
| *E. coli* | 1.49 ± 0.26 | 0.46 ± 0.27 | 0.075 ± 0.015 |
| *S. cerevisiae*[a] | 1.20 | 0.80 | – |
| *P. chrysogenum*[b] | 1.84 ± 0.08 | 0.38 ± 0.11 | 0.033 ± 0.012 |

The error ranges with a 95% confidence level were reported.

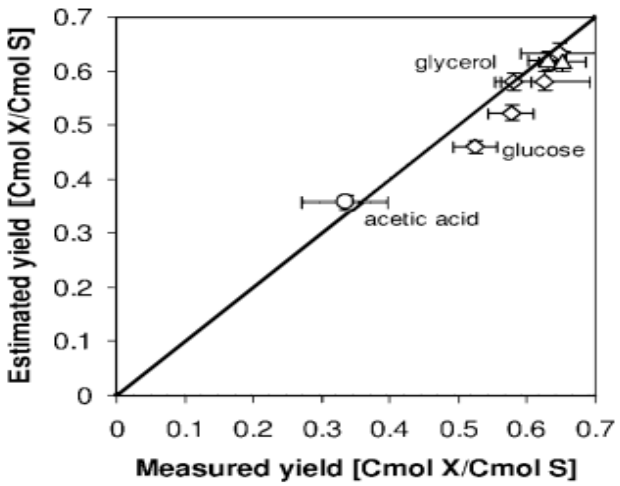


**Figure 1.**Biomass yields on substrates were compared using the most accurate ATP-stoichiometry parameter estimates (diamonds: glucose-limited, triangles: glycerol-limited, and circle: acetate-limited).

We were able to use CDR analysis to determine fluxes across the E. coli metabolic network at the same time as fluxes for glucose (glycerol) and acetate growth and KX (glucose) growth (see Supplementary Material for fluxes). One percent diluting is used in Figure 2 to show the flow distribution through central carbon metabolism, resulting in an hourly increase of 0.114. Under glucose-limited conditions, researchers have shown that glycolysis and PPP are partitioned unevenly at the G6P node. At D 14 0.1 h 1, this ratio was found to vary between 28 and 72 percent. Schmid et al. (2004) found that (Chassagnole and colleagues, 2002). In a year or two (Schmid and colleagues, 2004). There were 55%/20% splits between ICL and IDH in terms of fluxes converted to molecular units. See Figure 2 for an example of this. D 14 0.11 h 1 values of 53% / 21% for E. coli K12 are consistent with these results (Zhao and Shimizu, 2003). In the isocitrate dehydrogenase process, understanding how NADH and NADPH interact may have resulted in a 71 percent and a 13 percent flow to ketoglutarate and glyoxylate, respectively, according to Pramanik and Keasling (1997). Reduced glycerol consumption is possible by 13 percent by changing the flow of fructose biphosphatase (FBP) (Fig. 2). It has been reported by Holms (1996) that 13dPG consumes up to 80% of the glycerol in batch cultures of E. coli ML308 located at the G3P junction.

## Personal ties Bind Herbert and Pirt together

Exploring how growth, maintenance, and product production differ in terms of substrate consumption, using a black box model (growth and product formation rates). The parameters of these relationships include the maximum biomass and product yield coefficients, as well as the maintenance coefficient. The usage of oxygen and the creation of carbon dioxide may be linked. A metabolic model may be used to create these linear correlations (Van Gulik et al., 2001). These equations are shown in Table IX for each of the three carbon

sources evaluated. The variance of m is inversely proportional to the magnitude of M, and vice versa. The greatest biomass yields were 0.66 Cmol X/C Mol glucose, 0.70 Cmol X/C Mol glycerol, and 0.39 Cmol X/C Mol acetate from the substrates studied. At their greatest yields, the three glycerols had X/O2 ratios of 2.27, 1.71, and 0.69%, whereas the acetate had X/CO2 ratios of 1.93, 2.36, and 0.65%.

## CONCLUSIONS

By employing a large genome-scale model with well-defined parameters, it was feasible to develop fundamental metabolic network models. The stoichiometry of glucose, glycerol, and acetate for E. coli K12 was studied in aerobic substrate-limited chemostats utilizing the most basic models at different dilution rates.. Flow rates were considered since cell lysis was high (10–25 percent) in chemostats. The plants were grown using chemostats. Also included in the metabolic networks were data on protein concentration and the link between RNA and DNA, and growth rate. Additionally, the biomass's lipid and carbohydrate composition was considered.

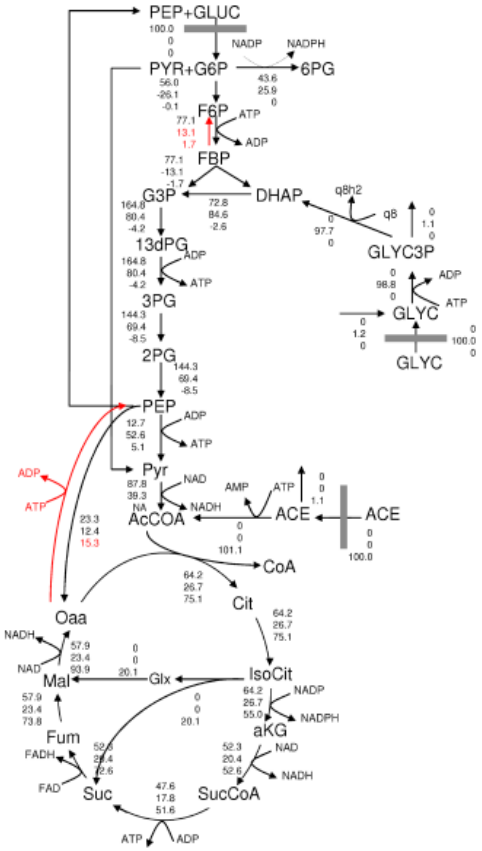


**Figure 2.**E. coli was grown anaerobically on glucose, glycerol and acetate at the 0.01 h dilution rate to evaluate the flow patterns of basic carbon. As a function of substrate absorption rate, all fluxes are displayed. Glycerol and acetate are rising in the first and second graphs. When comparing growth on glucose to growth on acetate, this is precisely the reverse of what one would anticipate to find.

A Herbert–Pirt relationship for each substrate is constructed using E. coli metabolic networks (all rates are presented in mol/CmolX/h).

| Substrate | Herbert-Pirt relations | | |
|---|---|---|---|
| Glucose | $-q_S = 0.25\mu + 0.0036$ | $-q_{O_2} = 0.44\mu + 0.022$ | $q_{CO_2} = 0.52\mu + 0.022$ |
| Glycerol | $-q_S = 0.47\mu + 0.0066$ | $-q_{O_2} = 0.58\mu + 0.023$ | $q_{CO_2} = 0.42\mu + 0.020$ |
| Acetate | $-q_S = 1.27\mu + 0.018$ | $-q_{O_2} = 1.46\mu + 0.023$ | $q_{CO_2} = 1.54\mu + 0.036$ |

The mass of biomass was calculated by the measurement of various constituents within it. The CDR approach may be used to estimate a metabolic network for aerobic carbon-limited E. coli K12 development, utilizing growth rate and biomass composition accuracy as input variables. d, KXs, and mATP were shown to be valid in-vivo estimations when compared to other animal data. It was previously believed that the rate of growth and the substrate were unrelated. The network model was able to compute all flows using just m as an input. The flow patterns and split ratios of the three substrates were found to be in excellent accord with previous studies. The metabolic network model is able to calculate the maximal biomass yields from the substrate using Herbert–Pirt relationships. Gert van der Steen deserves particular recognition for his contributions to the elemental analysis of biomass. A grant from the Flanders Institute for the Promotion of Innovation through Science and Technology (IWT-SBO) funded MEMORE (040125). (IWT Vlaanderen). The KluyverCenter for Genomics of Industrial Fermentation carried out this research as part of the Netherlands Genomics Initiative/Netherlands Organization for Scientific Research.

### Relationship between Biomass Composition and RQ for Cultures that Use Glucose as Substrate in the Appendix

When no products are formed, the carbon balance is expressed as follows:

$$q_{CO_2} + \mu = 6q_S \qquad (6)$$

as well as the broad balance of decrease

$$24q_S - 4q_{O_2} = \gamma_x\mu \qquad (7)$$

To calculate the respiratory quotient (RQ), the formula is: qCO2=qO2. Y 14 m=qS results when this information is combined with the measured biomass yield.

$$\gamma_x = \frac{4}{Y}\left[6 - \frac{6 - Y}{RQ}\right] \qquad (8)$$

According to Equation (8), Y, gx, and RQ all have a direct effect on biomass production (Y). Even if no byproducts are formed, the present offgas measurements and biomass production metrics may still tell us how much biomass is lost. If, for example, the average yield is 3 Cmol X/mol glucose and the RQ 14 1.05 value is used in aerobic E. coli chemostat cultures with glucose restriction, the output is gx14 4.2.

## REFERENCES


1. Ballesta JP, Schaechter M. 1972. Dependence of the rate of synthesis of phosphatidylethanolamine and phosphatidylglycerol on the rate of growth of Escherichia coli. J Bacteriol 110(1):452–453.
2. Bratbak G, Dundas I. 1984. Bacterial dry matter content and biomass estimations. Appl Environ Microbiol 48(4):755–757.
3. Bremer H, Dennis PP. 1996. Modulation of chemical composition and other parameters of the cell by growth rate. In: Neidhardt FC, Curtiss R, Ingraham JL, Lin ECC, Low KB, Magasanik B, Reznikoff WS, Riley M, Schaechter M, Umbarger HE, editors. Escherichia coli and Salmonella. Cellular and molecular biology. Washington, DC: American Society for Microbiology. p. 1527–1542.
4. Burgard AP, Vaidyaraman S, Maranas CD. 2001. Minimal reaction sets for Escherichia coli metabolism under different growth requirements and uptake environments. BiotechnolProgr 17(5):791–797.
5. Calhoun MW, Oden KL, Gennis RB, de Mattos MJ, Neijssel OM. 1993. Energetic efficiency of Escherichia coli: Effects of mutations in components of the aerobic respiratory chain. J Bacteriol 175(10):3020–3025.
6. Carson D, Pieringer RA, Daneo-Moore L. 1979. Effect of growth rate on lipid and [7] [7] lipoteichoic acid composition in Streptococcus faecium. BiochimBiophysActa 575(2):225–233.
7. Chassagnole C, Noisommit-Rizzi N, Schmid JW, Mauch K, Reuss M. 2002. Dynamic modeling of the central carbon metabolism of Escherichia coli. BiotechnolBioeng 79(1):53–73.
8. Durot M, Bourguignon PY, Schachter V. 2009. Genome-scale models of bacterial metabolism: Reconstruction and applications. FEMS Microbiol Rev 33(1):164–190.
9. Edwards JS, Palsson BO. 2000. The Escherichia coli MG1655 in silico metabolic genotype: Its definition, characteristics, and capabilities. ProcNatlAcadSci USA 97(10):5528–5533.
10. Emmerling M, Dauner M, Ponti A, Fiaux J, Hochuli M, Szyperski T, Wu¨thrich K, Bailey JE, Sauer U. 2002. Metabolic flux responses to pyruvate kinase knockout in Escherichia coli. J Bacteriol 184(1):152– 164.
11. Farmer IS, Jones CW. 1976. The energetics of Escherichia coli during aerobic growth in continuous culture. Eur J Biochem 67(1):115–122.
12. Feist AM, Henry CS, Reed JL, Krummenacker M, Joyce AR, Karp PD, Broadbelt LJ, Hatzimanikatis V, Palsson BO. 2007. A genome-scale metabolic reconstruction for Escherichia coli K-12 MG1655 that accounts for 1260 ORFs and thermodynamic information. MolSystBiol 3:121.
13. Fischer E, Sauer U. 2003. A novel metabolic cycle catalyzes glucose oxidation and anaplerosis in hungry Escherichia coli. J BiolChem 278(47): 46446–46451.
14. Han L, Enfors SO, Haggstrom L. 2003. Escherichia coli high-cell-density culture: Carbon mass balances and release of outer membrane components. Bioprocess BiosystEng 25(4):205–212. Table IX.
15. Herbert–Pirt relations derived from the constructed E. coli metabolic networks for each substrate (all rates are expressed in mol/CmolX/h).
16. BiotechnolBioeng 60(2):230–238. Reed JL, Vo TD, Schilling CH, Palsson B. 2003.
17. An expanded genome-scale model of Escherichia coli K-12. Genome Biol4:R54. Sauer U, Lasko DR, Fiaux J, Hochuli M, Glaser R, Szyperski T, Wuthrich K, Bailey JE. 1999.
18. Metabolic flux ratio analysis of genetic and environmental modulations of Escherichia coli central carbon metabolism. J Bacteriol 181(21):6679–6688. Schaub J, Mauch K, Reuss M. 2008.
19. Metabolic flux analysis in Escherichia coli by integrating isotopic dynamic and isotopic stationary 13C labeling data. BiotechnolBioeng 99(5):1170–1185.
20. Schmid JW, Mauch K, Reuss M, Gilles ED, Kremling A. 2004. Metabolic design based on a coupled gene expression-metabolic network model of tryptophan production in Escherichia coli. MetabEng 6(4):364– 377.
21. Schmidt K, Nielsen J, Villadsen J. 1999. Quantitative analysis of metabolic fluxes in Escherichia coli, using two-dimensional NMR spectroscopy and complete isotopomer models.
22. JBiotechnol 71(1–3):175–189. Siddiquee KAZ, Arauzo-Bravo MJ, Shimizu K. 2004. Metabolic flux analysis of pykF gene knockout Escherichia coli based on 13C-labeling experiments together with measurements of enzyme activities and intracellular metabolite concentrations.
23. ApplMicrobiolBiotechnol 63(4):407– 417. Stahlberg H, Muller DJ, Suda K, Fotiadis D, Engel A, Meier T, Matthey U, Dimroth P. 2001. Bacterial Naþ-ATP synthase has an undecameric rotor. EMBO Rep 2(3):229–233. Stouthamer A. 1973.
24. A theoretical study on the amount of ATP required for synthesis of microbial cell material. Antonie van Leeuwenhoek 39(3): 545–565. Sud IJ, Schaechter M. 1964. Dependence of the content of cell envelopes on the growth rate of Bacillus megaterium. J Bacteriol 88:1612–1617. Taymaz-Nikerel H, de Mey M, Ras C, ten Pierick A, Seifar RM,

25. van Dam JC, Heijnen JJ, van Gulik WM. 2009. Development and application of a differential method for reliable metabolome analysis in Escherichia coli. Anal Biochem 386(1):9–19.

26. van der Heijden RTJM, Heijnen JJ, Hellinga C, Romein B, Luyben KCAM. 1994. Linear constraint relations in biochemical reaction systems. I. Classification of the calculability and the balanceability of conversion rates. BiotechnolBioeng 43(1):3–10.

27. Van Gulik WM, Heijnen JJ. 1995. A metabolic network stoichiometry analysis of microbial growth and product formation. BiotechnolBioeng 48(6):681–698.

28. Van Gulik WM, de Laat WTAM, Vinke JL, Heijnen JJ. 2000. Application of metabolic flux analysis for the identification of metabolic bottlenecks in the biosynthesis of penicillin-G. BiotechnolBioeng 68(6):602–618.

29. Van Gulik WM, Antoniewicz MR, deLaat WTAM, L VJ, Heijnen JJ. 2001. Energetics of growth and penicillin production in a high-producing strain of Penicilliumchrysogenum. BiotechnolBioeng 72(2):185–193.

30. Varma A, Palsson BO. 1993. Metabolic capabilities of Escherichia coli. II. Optimal growth patterns. J TheorBiol 165(4):503–522. Verduyn C, Postma E, Scheffers WA,

31. vanDijken JP. 1992. Effect of benzoic acid on metabolic fluxes in yeasts: A continuous-culture study on the regulation of respiration and alcoholic fermentation. Yeast 8(7):501– 517.

32. Verheijen PJT. 2010. Data reconciliation and error detection. In: Smolke CD, editor. The metabolic pathway engineering handbook. Fundamentals. Boca Raton, FL: CRC Press. Zhao J, Shimizu K. 2003.

33. Metabolic flux analysis of Escherichia coli K12 grown on 13C-labeled acetate and glucose using GC-MS and powerful flux calculation method. J Biotechnol 101(2):101–117.

Citation: HuanLinyan, Yu Li, A. Malyska, " Based on Genome-Derived Minimal Metabolic Models of MG1655 Escherichia Coli, the in-Vivo Respiratory ATP Stoichiometry", American Research Journal of Biotechnology, Vol 1, no. 1, 2022, pp. 15-23.